Low-energy fixed points of random Heisenberg models

Y.-C. Lin
Institut für Physik, WA 331, Johannes Gutenberg-Universität, 55099 Mainz, Germany

R. Mélin
Centre de Recherches sur les Trés Basses Températures, B.P. 166, F-38042 Grenoble, France

H. Rieger
Theoretische Physik, Universität des Saarlandes, 66041 Saarbrücken, Germany

F. Iglói
Research Institute for Solid State Physics and Optics, H-1525 Budapest, P.O. Box 49, Hungary
and Institute of Theoretical Physics, Szeged University, H-6720 Szeged, Hungary
(Received 18 November 2002; revised manuscript received 3 March 2003; published 30 July 2003)

The effect of quenched disorder on the low-energy and low-temperature properties of various two- and three-dimensional Heisenberg models is studied by a numerical strong disorder renormalization-group method. For strong enough disorder we have identified two relevant fixed points, in which the gap exponent, ω, describing the low-energy tail of the gap distribution $P(\Delta)\sim\Delta^{\omega}$ is independent of disorder, the strength of couplings, and the value of the spin. The dynamical behavior of nonfrustrated random antiferromagnetic models is controlled by a singletlike fixed point, whereas for frustrated models the fixed point corresponds to a large spin formation and the gap exponent is given by $\omega\approx 0$. Another type of universality class is observed at quantum critical points and in dimerized phases but no infinite randomness behavior is found, in contrast to that of one-dimensional models.

DOI: 10.1103/PhysRevB.68.024424 PACS number(s): 75.10.Nr, 75.10.Jm, 75.40.Gb

I. INTRODUCTION

The Heisenberg model plays a central role in the theory of magnetic ordering[1] and the two-dimensional (2D) antiferromagnetic (AF) model has been intensively studied motivated by its relation to high-temperature superconductivity.[2] According to the Mermin-Wagner theorem,[3] no long-range order (LRO) can persist at finite temperatures in the homogeneous Heisenberg model if $d\leqslant 2$. At zero temperature, the LRO of the classical ground state is reduced by quantum fluctuations. This effect is particularly strong in (quasi)-1D AF models and gives rise to the complete destruction of Néel-type LRO. Fluctuations enhanced by quenched randomness and frustration can further destabilize LRO, resulting in disordered ground states even in higher-dimensional systems. In various experiments, in which quasi-two-dimensional magnetic materials that can appropriately be described by the 2D Heisenberg antiferromagnet (HAF) model were diluted with static nonmagnetic impurities (Mg or Zn in La_2CuO_4, and Mg in K_2CoF_4 or K_2MnF_4), a disorder-induced transition from Néel order to a spin liquid was observed: If the impurity concentration is larger than a critical value the LRO is destroyed.[4,5]

The behavior of HAFs in the presence of quenched randomness is generally very complex and present understanding of this is not complete. Most of the theoretical results have been obtained for 1D models, many of them by a strong disorder renormalization-group (SDRG) method introduced originally by Ma, Dasgupta, and Hu for the random $S=1/2$ AF spin chain.[6] Fisher[7] has shown that the SDRG method leads to asymptotically exact results in the vicinity of a quantum critical point, which corresponds to the chain without dimerization. At the quantum critical point, the ground state can be described by the notion of a random singlet (RS) phase, which consists of effective singlets of pairs of spins that are arbitrarily far from each other. Fisher's SDRG treatment has been extended to the dimerized phases that turned out to be equivalent to quantum Griffiths phases.[8] The SDRG method has also been applied for random $S=1$ (Ref. 9) and $S=3/2$ (Ref. 10) spin chains and for various random spin ladder models.[11] In general, the Haldane gapped phases stay gapped for weak disorder, while they become gapless and often form RS phases for strong disorder.

To study the singular properties of the $S=1/2$ Heisenberg model with mixed ferromagnetic (F) and AF couplings, the SDRG method has to be modified. In one dimension, the presence of ferromagnetic couplings leads to the formation of large spin clusters in the renormalization-group (RG) treatment, with an effective moment that grows without limits as the energy scale is lowered.[12] As a consequence, the ground-state properties of random Heisenberg chains with mixed AF and F couplings and of those with only AF couplings are different. The presence of large effective spins in the low-energy limit was also observed for random AF spin ladders with site dilution.[13]

Not many theoretical investigations of the effect of quenched disorder in higher-dimensional random HAFs exist, and those that have been done are almost exclusively restricted to dilution on the square lattice. Quantum Monte Carlo studies of the HAF on a diluted square lattice show that LRO disappears at the classical percolation point.[14] While in earlier investigations a unique, *S*-dependent critical

behavior was found,[14] recent studies identify the transition as an S-independent classical percolation transition with well-known exponents.[15] Another work studied the $\pm J$ Heisenberg (quantum) spin glass and found that for a concentration of F bonds $p > p_c \approx 0.11$ the Néel-type LRO in the ground state vanishes and is replaced by a so-called spin-glass phase.[16] Within the spin-glass phase, the average ground-state spin, S_{tot}, scales as $S_{\mathrm{tot}} \sim \sqrt{N}$, and the gap as $\Delta E \sim 1/N$, where N is the number of spins.[17]

In this paper we study the effect of randomness in higher-dimensional HAFs by means of the SDRG method. In particular, we consider the low-energy behavior of frustrated and nonfrustrated systems in two and three dimensions. As we mention in the next section the pure (i.e., nonrandom) versions of these models have a ground state that has either AF or dimer LRO or is disordered, i.e., in a spin-liquid state. By calculating the gap distribution and cluster formation within the SDRG scheme we characterize the change of the ground-state structure of the pure systems by the effect of the disorder.

The paper is organized as follows: The models and their phase diagrams for nonrandom couplings are presented in Sec. II. The SDRG method and its different low-energy fixed points for (quasi)-1D systems are discussed in Sec. III. Results of the SDRG method on different 2D and 3D models are presented in Sec. IV and discussed in Sec. V.

II. THE MODELS AND THEIR PHASE DIAGRAM FOR NONRANDOM COUPLINGS

We start with the Hamiltonian of a nearest-neighbor spin-1/2 AF Heisenberg model,

$$H_1 = \sum_{\langle kk' \rangle\ \mathrm{nn}} J \mathbf{S}_k \mathbf{S}_{k'}, \tag{1}$$

where $J > 0$ and the summation runs over nearest-neighbor (nn) pairs, $\langle k,k' \rangle$, of a regular lattice. In one dimension, Néel-type LRO is destroyed by quantum fluctuations and the system with half-integer spin value S shows quasi-long-range order (QLRO), i.e., correlations in the ground state decay algebraically.[18,19] A similar behavior can be observed in AF spin ladders with an odd number of legs.[20] Both systems have a gapless excitation spectrum and in finite chains of length L the gap vanishes algebraically with a dynamical critical exponent $z_c = 1$, which is characteristic for a quantum critical point:

$$\Delta E_{\mathrm{cr}}(L) \sim 1/L^{z_c}. \tag{2}$$

Quantum fluctuations play a different role in AF spin chains with an integer spin[19] and for spin ladders with an even number of legs.[20] These systems show a topological string order, which is accompanied by exponentially decaying correlations and by a finite gap in the spectrum.

One can approach a 2D geometry by successively increasing the number of legs of AF spin ladders. The resulting square lattice has a qualitatively different low-energy behavior: The effect of quantum fluctuations is weaker and the ground state shows Néel-type LRO.[21] Compared with the classical ground state the sublattice magnetization for $S = 1/2$ is reduced by about 40%. Generally in ordered AF phases the excitation spectrum is gapless. In a finite d-dimensional system of linear size L—according to spin-wave theory and analysis of the nonlinear sigma model—the gap behaves as[22]

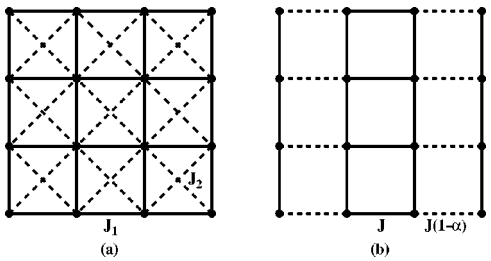

FIG. 1. (a) The J_1-J_2 model and (b) the dimerized model on the square lattice.

$$\Delta E_{\mathrm{od}}(L) \sim 1/L^d. \tag{3}$$

Frustration generally leads to a further reduction of the Néel LRO. Frustration of geometrical origin is present in the triangular lattice, where the sublattice magnetization is about 50% of its classical value.[23] In more loosely packed frustrated lattices, such as in the *kagomé* lattice,[24] the square lattice with crosses[25] (see, however, Ref. 26), or in the 3D pyrochlore lattice,[27] the LRO completely disappears and the systems have a disordered ground state. The correlations are short ranged and one finds a finite triplet gap in which a continuum of singlet excitations exists. In the case of the *kagomé* lattice these extend down to the ground state.[24]

Competing interactions are another source of frustration which can also lead to disordered ground states. As an example, we consider the AF J_1-J_2 model with first- (J_1) and second- (J_2) neighbor interactions, described by the Hamiltonian

$$H = H_1 + H_2, \tag{4}$$

where

$$H_2 = \sum_{\langle kk' \rangle\ \mathrm{nnn}} J_2 \mathbf{S}_k \mathbf{S}_{k'}, \tag{5}$$

and the coupling in H_1 [Eq. (1)] is denoted as $J \equiv J_1$ [see Fig. 1(a)]. In two dimensions, there are at least three phases, as shown in Fig 2(a). For small frustration, $J_2/J_1 = \rho$, the system possesses AF LRO, whereas for large frustration the system goes to the collinear state, in which ferromagnetically ordered columns of spins are arranged antiferromagnetically. In the range $0.34 < \rho < 0.60$, the ground state is disordered and the spectrum is gapped for all types of excitations.[28,29] According to recent numerical studies[30] there are probably several quantum phases in this region, separated by different types of quantum phase transitions.

Finally, we introduce a dimerization into model (1). We consider the square lattice, denote a lattice site k by its two coordinates, $k = (i,j)$, and define

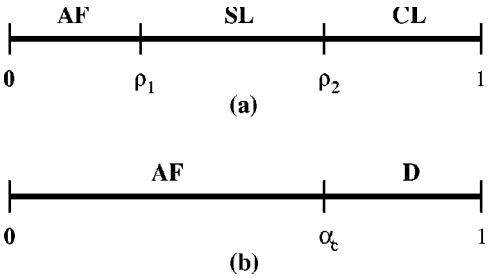

FIG. 2. Phase diagrams of square lattice HAF models. (a) For the J_1-J_2 model with varying frustration, $\rho = J_2/J_1$, there are three regions: the ordered AF phase and the ordered collinear (CL) phase, separated by a disordered spin-liquid (SL) region. (b) In the dimerized model, the AF and dimer (D) ordered phases are separated by a quantum critical point at α_c.

$$H_{\rm dim} = -\sum_{i,j} J\alpha \mathbf{S}_{2i,j}\mathbf{S}_{2i+1,j}. \tag{6}$$

The dimerized model is then described by the Hamiltonian $H = H_1 + H_{\rm dim}$ and has a layered structure, see Fig. 1(b). Its phase diagram is shown in Fig. 2(b) as a function of the dimerization parameter $0 < \alpha < 1$. For $\alpha < \alpha_c = 0.686$ the ground state has AF LRO, whereas for $\alpha > \alpha_c$ the system is in an ordered dimerized phase, in which spin-spin correlations along horizontal lines approach different limits if the distance between the spins is odd or even, respectively. In the dimerized phase, there is a finite gap which vanishes at α_c as $\Delta E \sim (\alpha - \alpha_c)^{\nu}$ with $\nu = 0.71$, characteristic for the universality class of the 3D classical Heisenberg model.[31,32] We note that dimerization with another topology has been studied recently in Ref. 33.

The random Heisenberg models we investigate in this paper include the 2D/3D AF model on the regular lattice (1), the dimerized AF model (6) in two dimensions, geometrically frustrated AF models on the triangular lattice as well as on the *kagomé* lattice, the 2D/3D J_1-J_2 model, and the 2D/3D AF-F models. We are interested in how the phase diagrams in Fig. 2 are modified due to the presence of strong quenched randomness.

III. THE SDRG METHOD AND ITS LOW-ENERGY FIXED POINTS IN 1D MODELS

The basic ingredient of the SDRG method in Heisenberg models is a successive decrease of the energy scale of excitations via a successive decimation of couplings. We start with a $S = 1/2$ HAF model in which the strongest coupling is, say, J_{23}, the one between lattice sites 2 and 3 (cf. Fig. 3). If J_{23} is much larger than its neighboring couplings J_{12}, J_{13}, J_{24}, and J_{34}, the spins at 2 and 3 form an effective singlet and are decimated. The effective coupling between the remaining sites 1 and 4 in second-order perturbation theory is given by

$$\tilde{J}_{14}^{\rm eff} = \lambda \frac{(J_{12} - J_{13})(J_{34} - J_{24})}{J_{23}}, \quad \lambda(S = 1/2) = 1/2. \tag{7}$$

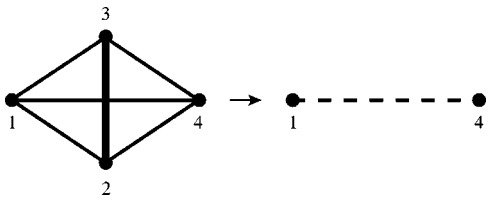

FIG. 3. Singlet formation and decimation for a spin configuration that does not have a chain topology and typically occurs in higher-dimensional systems.

In a chain geometry the couplings J_{13} and J_{24} would not be present and the resulting RG flow always generates AF couplings. However, for extended, not strictly 1D objects, some of the generated new couplings can be ferromagnetic (e.g., if $J_{12} < J_{13}$ and $J_{34} > J_{24}$ or vice versa) and therefore the decimation rules have to be extended. If at one RG step an F bond turns out to be the strongest one, its decimation will lead to an effective spin $\tilde{S} = 1$. In the following steps, the system will renormalize to a set of effective spins of different magnitude interacting via F *and/or* AF couplings.

For higher-dimensional systems, the basic decimation processes are the singlet formation in Eq. (7) and the effective spin (cluster) formation. To specify the latter, let us consider three spins S_1, S_2, and S_3 with interactions fulfilling $|J_{23}| \gg |J_{12}|, |J_{13}|$. In the action of the RG, the two original spins S_2 and S_3 form a new effective spin of magnitude $\tilde{S} = |S_2 \pm S_3|$ representing the total spin of the ground state in the two-spin Hamiltonian $H_{23} = J_{23}\mathbf{S}_2\mathbf{S}_2$, where the positive (negative) sign refers to an F (AF) coupling. The corresponding energy gap, Δ, between the ground state and the first excited state in the Hamiltonian H_{23} is given by $\Delta = |J_{23}|(S_2 + S_3)$ and $\Delta = J_{23}(|S_2 - S_3| + 1)$, for an F and AF coupling, respectively. If $J_{23} > 0$ (AF) and $S_2 = S_3$, it follows an effective singlet formation as described above. If $\tilde{S} \neq 0$, within first-order perturbation theory the new coupling between S_1 and $\tilde{S}_{23}$ is given by

$$\tilde{J}^{\rm eff} = c_{12}J_{12} + c_{13}J_{13}, \tag{8}$$

with

$$c_{12} = \frac{\tilde{S}(\tilde{S}+1) + S_2(S_2+1) - S_3(S_3+1)}{2\tilde{S}(\tilde{S}+1)}$$

and

$$c_{13} = \frac{\tilde{S}(\tilde{S}+1) + S_3(S_3+1) - S_2(S_2+1)}{2\tilde{S}(\tilde{S}+1)}.$$

At each RG step, we find the pair of the spins with the largest energy gap Δ that sets the energy scale, Ω, and decimate them according to renormalization rules described in Eqs. (7) or (8). A detailed derivation of these renormalization rules can be found in Ref. 34.

The fixed point of the RG transformation for lattices that do *not* have a chain geometry may depend on their topology, the original distribution of bonds, the strength of the disorder, etc. We briefly summarize the existing results for spin

chains and ladders since it might be helpful for analyzing the RG results in higher-dimensional systems.

In the case of the random AF chain (which has neither F bonds nor frustration), the RG procedure described above runs into an infinite randomness fixed point (IRFP) corresponding to a random singlet phase. In this phase the renormalized clusters are singlets, thus the total magnetic moment is zero, and the energy and length scales are related via

$$-\ln \Omega \sim L^{1/2}, \tag{9}$$

which means that the dynamical exponent is formally infinite.

A dimerized $S=1/2$ chain with random AF even (J_e) and odd (J_o) couplings shows dimer order, and the low-energy behavior is controlled by a random dimer (RD) fixed point at which the dynamical exponent, z, is finite and a continuously varying function of the strength of the dimerization measured by $\delta_{\rm dim}=[\ln J_e]_{\rm av}-[\ln J_o]_{\rm av}$.[8,35] At this fixed point, the low-energy tail of the distribution of the effective couplings, J_e, is given by

$$P(J_e,\Omega)\mathrm{d}J_e \simeq \frac{1}{z}\left(\frac{J_e}{\Omega}\right)^{-1+1/z}\frac{\mathrm{d}J_e}{\Omega}, \tag{10}$$

for $\delta_{\rm dim}>0$. This random dimer phase is a Griffiths phase[36] and we refer to it as a Griffiths fixed point (GFP). At this GFP, the gap of finite chains of length L obeys a distribution similar to Eq. (10):

$$P_L(\Delta)=L^z\tilde{P}(L^z\Delta)\sim L^{z(1+\omega)}\Delta^{\omega}, \tag{11}$$

which is characterized by the gap exponent, ω. As a consequence of Eq. (11), which holds in any dimension, several dynamical quantities at a GFP are singular and the characteristic exponents can all be expressed via ω. For example, the susceptibility χ, the specific heat C_v (at a small temperatures T), and the magnetization m (in a small field h) behave as

$$\chi(T)\sim T^{-\omega}, \quad C_v(T)\sim T^{\omega+1}, \quad m(h)\sim h^{\omega+1}. \tag{12}$$

In the Griffiths phase there is a simple relation between the dynamical exponent, z, and the gap exponent, ω, which can be obtained by the following phenomenological consideration.[37] If the Griffiths singularities are due to rare events (produced by the couplings) that give rise to *localized* low-energy excitations, the gap distribution should be proportional to the volume, $P_L(\Delta)\sim L^d$. From Eq. (11) it then follows that

$$z=\frac{d}{1+\omega}, \tag{13}$$

which is consistent with the exact result in the random dimer phase in Eq. (10). However, if the low-energy excitations are *extended* the relation (13) might not hold.

In a spin chain with mixed F and AF couplings,[12] large effective spins, $S_{\rm eff}$, are formed at the fixed point of the transformation. The size of these spin clusters scales with the fraction of surviving sites during decimation, $1/N$, as

$$S_{\rm eff}\sim N^{\zeta}. \tag{14}$$

The following random-walk argument[12] gives $\zeta=1/2$. The total moment of a typical cluster of size N can be expressed as $S_{\rm eff}=|\Sigma_{1=1}^{N}\pm S_i|$, where neighboring spins with F (AF) couplings enter the sum with the same (different) sign. If the positions of the F and AF bonds are uncorrelated and if their distribution is symmetrical, one has $S_{\rm eff}\propto N^{1/2}$, i.e., Eq. (14) with $\zeta=1/2$.

A nontrivial relation constitutes the connection between the energy scale Ω and the size of the effective spin,

$$S_{\rm eff}\sim \Omega^{-\kappa}, \tag{15}$$

where a numerical estimate of the exponent is $\kappa=0.22(1)$.[12] Comparing Eq. (14) with Eq. (15), the relation between the length scale $L\sim N^{1/d}$ ($d=1$) and the energy scale is

$$\Omega\sim L^{-z}, \quad z=\frac{d\zeta}{\kappa}=\frac{1}{2\kappa}, \tag{16}$$

where z is the dynamical exponent. The distribution of low-energy gaps, $P_L(\Delta)$, has the same power-law form as in Eq. (11). Therefore from the scaling behavior of $P_L(\Delta)$ the gap exponent, ω, and the dynamical exponent, z, can be obtained. Due to the large moment formation the singularities of the dynamical quantities are different from those in the random dimer phase in Eq. (12), i.e., at a GFP. Generalizing the reasoning in Ref. 12, we obtain in d dimensions

$$\chi(T)\sim T^{-1},\ C_v(T)\sim T^{2\zeta(\omega+1)}|\ln T|,$$
$$m(h)\sim h^{\zeta(1+\omega)/[1+\zeta(1+\omega)]}, \tag{17}$$

thus the singularities involve both exponents ζ and ω. In the following, we refer to this type of fixed point as a large spin fixed point (LSFP).

AF spin ladders, although being quasione dimensional, have a nontrivial, non-chain-like topology and during renormalization also F bonds can be generated according to Eq. (7). Different random AF two-leg ladders were studied in Ref. 11 with the following results. If the disorder is strong enough the gapped phases of the nonrandom systems become gapless. The low-energy behavior is generally controlled by a GFP, where the dynamical exponent is finite and depends on the strength of the disorder. However, at random quantum critical points, separating phases with different topological or dimer order, the low-energy behavior is controlled by an IRFP. In diluted AF spin ladders also LSFPs have been identified.[13]

To close this section we summarize that in one-dimensional and in quasi-one-dimensional random Heisenberg systems there are two different types of low-energy fixed points, which are expected to be present in higher-dimensional systems, too. Both for a GFP and for a LSFP, the low-energy excitations follow the same power-law form as in Eq. (11) from which the exponents, ω and z, can be deduced. At a GFP these two exponents are expected to be related through $z=d/(1+\omega)$ (13). On the other hand, for a LSFP, where the excitations are not localized, this relation probably does not hold. At such a LSFP there is a third independent exponent ζ involved in the dynamical singularities partially listed in Eq. (17).

In the next section we study different two- and three-dimensional random Heisenberg models. In particular, we are interested in the possible difference in the low-energy fixed point for nonfrustrated and frustrated systems. Since extended (quasione dimensional or higher dimensional) random HAF models and Heisenberg models with mixed F and AF bonds follow the same renormalization route, they could, in principle, be attracted by the same fixed points, but also new fixed points can emerge, as we show.

IV. RENORMALIZATION OF HIGHER-DIMENSIONAL SYSTEMS

This section is the central part of our work, where we present our results for the ground-state structure of various two- and three-dimensional random Heisenberg models obtained by the numerical application of the SDRG. In practice we start with a finite system of linear size L with periodic boundary conditions and perform the decimation procedure up to the last effective spin (or decimate out the last spin singlet). The energy scale corresponding to the last decimation step is denoted by Δ. This procedure is performed for several thousand realizations of the disorder and yields a histogram for Δ, which represents our estimate of the probability distribution $P_L(\Delta)$. From this we extract the gap exponent ω and the dynamical exponent z via the asymptotic relation given in Eq. (11). Moreover, from the average size of the effective spin at the last step, $\mu_L=[S_{\rm eff}]_{\rm av}$, the cluster exponent, ζ, in Eq. (14) is deduced. The value of ω, z, and ζ is then used to discriminate the different possible low-energy fixed points described in the previous section.

Throughout this paper we use a power-law distribution for the random couplings $0<J\leqslant 1$ for AF models:

$$P_D(J)=\frac{1}{D}J^{-1+1/D}, \tag{18}$$

where $D^2=[(\ln J)^2]_{\rm av}-[\ln J]^2_{\rm av}$ denotes the strength of the disorder. Note that both the initial distribution of the couplings in Eq. (18) and the final distribution of gaps in Eq. (11) follow power laws. If $1/(\omega+1)<D$, the strength of disorder is reduced during renormalization, thus the low-energy random fixed point is a conventional one. More generally, for a conventional random fixed point, $\omega>-1$. In contrast to this, at an IRFP the disorder growths without limits, thus here formally $\omega=-1$ and the dynamical exponent is infinite. We often use the uniform distribution, which corresponds to $D=1$ in Eq. (18). For models with random F and AF couplings we take either a Gaussian distribution

$$P_G(J)=\frac{1}{\sqrt{2\pi\sigma^2}}\exp(-J^2/2\sigma^2), \tag{19}$$

or a rectangular distribution

$$P_r(J)=\Theta(J-r+1/2)\Theta(r+1/2-J), \tag{20}$$

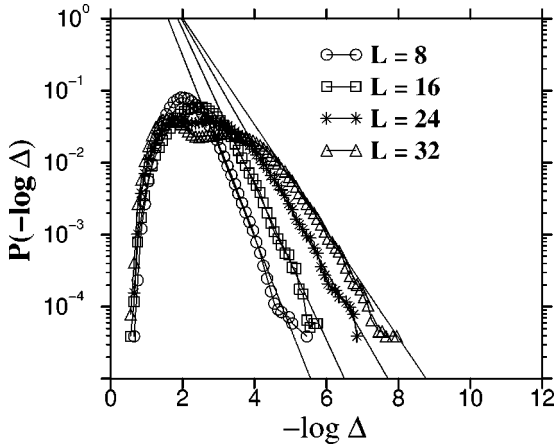

FIG. 4. Distribution of the energy gap of the square lattice HAF with uniformly distributed random couplings, for linear sizes $L=8,16,24$, and 32. The slope of the low-energy tail of the distributions is given by $-(\omega+1)=-d/z$. The straight line for $L=32$ has a slope ≈ -1.7.

where $\Theta(x)=1$, for $x>0$ and zero, otherwise. The latter distribution is symmetric for $r=0$, whereas for $r=1/2$ we recover the uniform distribution of AF couplings in Eq. (18) with $D=1$.

A. Two-dimensional models

In the calculations for two dimensions we usually considered systems of linear size up to $L=32$, but for some cases in which the convergence was faster we went only up to $L=10-16$. The typical number of realizations were several hundred thousands for the smaller sizes and several ten thousands for larger systems for each value of D. At the first part we investigate nonfrustrated models, such as the HAF on the square lattice with and without dimerization. In the second part of our study we consider frustration, the origin of which could be (i) geometrical such as, for instance, for the triangular and *kagomé* lattices (ii) due to a random mixture of F and AF couplings such as, for instance, for the $\pm J$ spin-glass model, and (iii) due to competition between first- and second-neighbor couplings such as for the J_1-J_2 model.

1. HAF on the square lattice

We start with the renormalization of the HAF on the square lattice. The probability distribution of the gap calculated for a uniform bond distribution [Eq. (18) with $D=1$] is shown in Fig. 4 for different linear sizes. In a log-log plot the small gap region of the curve is linear, the slope of which, according to Eq. (11), corresponds to $\omega+1$. With increasing size one observes a slight broadening of the distributions indicating a decreasing effective gap exponent which, however, seems to converge to a finite asymptotic value,

$$\omega_{AF}=0.7(1), \quad d=2. \tag{21}$$

During renormalization we observed simultaneously an effective singlet formation, thus in Eq. (14) one has $\zeta=0$. Our estimate for the dynamical exponent satisfies the relation in Eq. (13), yielding $z_{AF}=1.2$. Thus we conclude that the

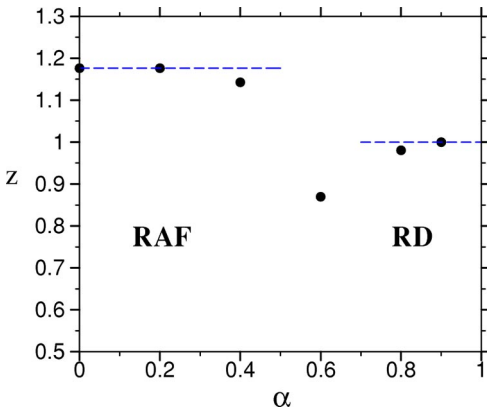

FIG. 5. Extrapolated dynamical exponent of the random dimerized HAF on the square lattice. The random AF and the random dimerized phases are separated by a crossover region in which the dynamical exponent is minimal.

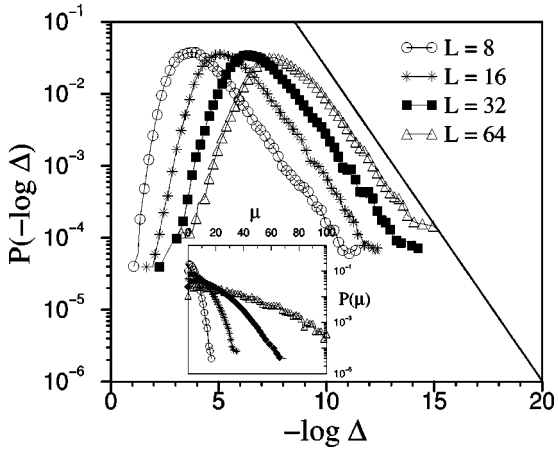

FIG. 6. Probability distribution of the energy gap on the square lattice with mixed F and AF bonds following a Gaussian distribution with $\sigma=1$. (The slope of the straight line is -1.) Inset: Distribution of the spin moments.

low-energy fixed point of the system is a *conventional, finite disorder* Griffiths fixed point and the thermodynamical singularities are given by Eq. (12). For other disorder strengths D we reach the same conclusions and our estimates for the gap exponents for each D agree with the value in Eq. (21) within the error bars. Thus the low-energy singular behavior of the 2D random HAF does not depend on the strength of disorder, in contrast to random quantum spin ladders.[11]

2. Square lattice HAF with dimerization

Next we study the low-energy behavior of the dimerized HAF, as sketched in Fig. 1(b). For site and bond dilution the stability of the gapped, dimerized phase was recently investigated.[38] Here we consider the effect of strong AF bond disorder. In our calculation we used uniform initial randomness and performed the renormalization for several values of the dimerization parameter, α. The possible values of the two types of couplings were in the regions (0,1) and $[0,(1-\alpha)]$, respectively. For any value of α in the range $0<\alpha<1$, we observed an effective singlet formation, and the estimated gap exponents ω and dynamical exponents z are found to satisfy the relation in Eq. (13). The extrapolated dynamical exponents as plotted in Fig. 5 seem to be approximately constant in two regions, which corresponds to the two phases of the pure model in Fig. 2(b). For weaker dimerization the dynamical exponent corresponds to the one of the random HAF, and for stronger dimerization z is approximately equal to the one of the disconnected two-leg ladder systems, to which the case $\alpha=1$ reduces, with $z\approx 1.07$.[11] We expect that the dimer order is finite in the RD region, whereas it is zero (or very small) in the random HAF region. Between the two regions, corresponding to the neighborhood of the phase-transition point in the pure system in Fig. 2(b), the dynamical exponent drops to a minimal value. This crossover could happen in a smooth, nonsingular way, or in a sharp phase transition separating the random AF and the random dimer phases. Due to strong finite-size effects we could not discriminate between the two scenarios.

We note that z in the crossover region behaves in the opposite way as that in the dimerized ladders, where the dynamical exponent at the transition point in a finite system is maximal, and increases without limits[11] for increasing system size, signaling an IRFP. In the two-dimensional case considered here the combined effect of critical fluctuations and quenched randomness seem to reduce the value of the dynamical exponent. Our calculations indicate that in the random dimer phase the low-energy behavior is controlled by a GFP and the dynamical singularities are given by Eq. (12).

3. Randomly frustrated models (two dimensions)

In this section we consider the Heisenberg model on the square lattice with a random mixture of F and AF couplings. This is a model for a quantum spin glass[16,17] and we denote the corresponding fixed point as the spin-glass fixed point (SGFP), although we do not explicitly check for the existence of proper spin-glass order in the ground state (for instance, via the calculation of the Edwards-Anderson spin-glass order parameter[39]). As we can see, this fixed point differs from the other fixed points we found for nonfrustrated models, so we feel that the use of this notation is justified. In particular, we find a large spin formation proportional to L during the RG procedure implying a ground-state spin $S\propto\sqrt{N}$, which is reminiscent of the spin-glass behavior found in (Refs. 16 and 17) for this model with alternative methods.

First we report the results for the Gaussian randomness in Eq. (19). For this case the distributions of the gaps and of the effective spin moments are shown in Fig. 6. The gap distributions for different finite sizes have a very similar structure: they are merely shifted to each other by a constant proportional to $\ln L$. The slope of the low-energy tail of the distributions is practically independent of the strength of disorder and in all cases the gap exponent is equal to

$$\omega_{SG}=0, \quad d=2, \tag{22}$$

within an accuracy of a few percent. From the finite-size scaling properties of the gap distribution, we infer that the relation in Eq. (13) is satisfied and therefore

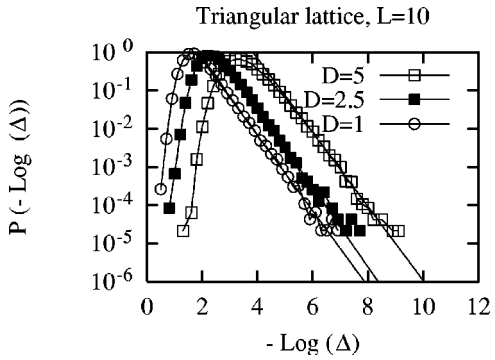

FIG. 7. Probability distribution of the energy gap for the triangular lattice HAF for different strength of randomness in Eq. (18). The low-energy tail of the distributions, which has practically no finite-size dependence for $L \geqslant 10$, is consistent with the same gap exponent, $\omega = 0$, implying a dynamical exponent $z_{SG} = d = 2$.

$$z_{SG} = 2, \quad d = 2, \tag{23}$$

within an accuracy of a few percent.

On the other hand, the distribution of the effective spin moments in the inset to Fig. 6 shows a tendency to broaden with increasing system size and its average value has a linear L dependence, $[\mu_L]_{\rm av} \approx .42L$. Therefore the moment exponent in Eq. (14) is

$$\zeta_{SG} = 1/2, \quad d = 2. \tag{24}$$

We have repeated the above analysis using the symmetric rectangular distribution in Eq. (20) both for the $S = 1/2$ and the $S = 1$ models, and we obtained the same critical exponents as those in the Gaussian case. Thus we can conclude that the low-energy behavior in randomly frustrated 2D models is controlled by the same SGFP, independent of the type of randomness and the size of the spin.

4. Geometrically frustrated models

In this section we consider the HAF on two geometrically frustrated lattices that have qualitatively different ground states in the nonrandom case. The triangular lattice has finite AF long-range order and low-energy excitations behave as those in Eq. (3). In contrast to this, the ground state of the *kagomé* lattice is disordered and the low-energy singlet excitations have a more complicated size dependence.

We start with the HAF on the triangular lattice using the power-law distribution in Eq. (18) for the random couplings. The distribution function of the gap is presented in Fig. 7 for different disorder strengths. The slope of the low-energy tail of the distributions is again, as for the randomly frustrated model of the last section, practically independent of the strength of disorder and in all cases the gap exponent is equal to $\omega = 0$ within an accuracy of a few percent.

When calculating the moment of the spin clusters, we notice large spin formation during the action of the RG. From the size dependence of the average moment we obtain the exponent in Eq. (14) to be $\zeta = 1/2$, independent of the strength of disorder. From the finite-size scaling properties of the gap distribution, we infer that the relation in Eq. (13) is satisfied and therefore $z_{SG} = d = 2$. Thus we can conclude that the thermodynamical quantities in the random triangular HAF obey the relations in Eq. (17).

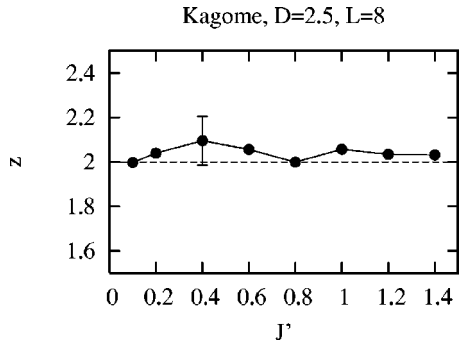

FIG. 8. Dynamical exponent of the random HAF on the dimerized *kagomé* lattice with a randomness parameter $D = 2.5$ calculated in finite systems having L^2 triangles, thus $3L^2$ sites. The connecting lines are guide to the eyes, and a typical error bar is also indicated.

Next we focus on the *kagomé* lattice and enlarge the parameter space by considering the dimerized model, as introduced in Ref. 40: Couplings in up-pointing triangles (J) are different from those in down-pointing triangles (J') (see Fig. 1 of Ref. 40). Analyzing the results of the RG calculation as already described for the triangular lattice, we obtain a set of gapped, dynamical, and moment exponents for different dimerizations, $0.1 < J'/J < 1.5$, and disorder strengths, $D = 1$, 2.5, and 5. In Fig. 8 we show our estimates for the dynamical exponents for $D = 2.5$, which are consistent with the SGFP result in Eq. (22). Also for other disorder strengths we find the same behavior and we conclude that the low-energy physics of the random *kagomé* HAF is controlled by the SGFP and the thermodynamic singularities are described by Eq. (17).

5. The J_1-J_2 model

In our final example for the 2D case, the source of frustration is the competition between first- —J_1—and second-neighbor—J_2—couplings, which obey a power-law distribution in Eq. (18) within the ranges of $0 < J_1 \leqslant J_1^{\rm max}$ and $0 < J_2 \leqslant J_2^{\rm max}$, respectively. We have performed the previous analysis at different points of the phase diagram, $J_2^{\rm max}/J_1^{\rm max}$, and for different strengths of disorder, D. In all cases we found that the relation in Eq. (13) is valid. As an illustration we show in Fig. 9 our estimates for the dynamical exponents for a disorder strength $D = 5/3$, which are consistent with the SGFP value in Eq. (22) in a wide range of $0.2 < J_2^{\rm max}/J_1^{\rm max} < 2.0$. The same conclusion holds for other disorder strengths in the range of $1 \leqslant D \leqslant 5$. During renormalization there is large spin formation and the calculated cluster exponent is consistent with $\zeta_{SG} = 1/2$. Thus we can conclude that in the J_1-J_2 model the different phases in the pure model (AF and CL ordered, disordered SL) are washed out by strong disorder, and the whole frustrated region, $J_2/J_1 > 0$, is controlled by the SGFP.

B. Three-dimensional models

For the calculations in three dimensions that we present now we considered only systems of linear sizes $L = 6,8,10$,

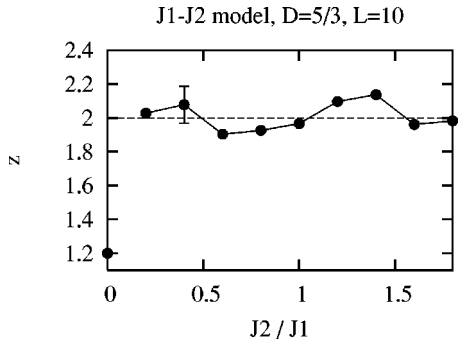

FIG. 9. Dynamical exponent of the J_1-J_2 model on the square lattice with a power-law randomness with $D=5/3$. The connecting lines are guide to the eyes, and a typical error bar is also indicated.

and 12, in some cases we went up to $L=16$. Larger system sizes were computationally not feasible. The typical number of realizations were several ten thousands for each point. Due to the smaller system sizes the finite-size effects in three dimensions are stronger than in two dimensions. These finite-size effects turned out to be too strong in the random HAF on the cubic lattice for a safe estimate for the gap exponent. We can, however, conclude that there is no large spin formation and the low-energy behavior is controlled by a conventional GFP.

1. Randomly frustrated models (three dimension)

We have studied models with mixed F and AF couplings for different forms of initial randomness (Gaussian, symmetric, and asymmetric rectangular) and for comparison, calculations on the $S=1$ model are also performed. The calculated distributions of the gaps are presented in Fig. 10.

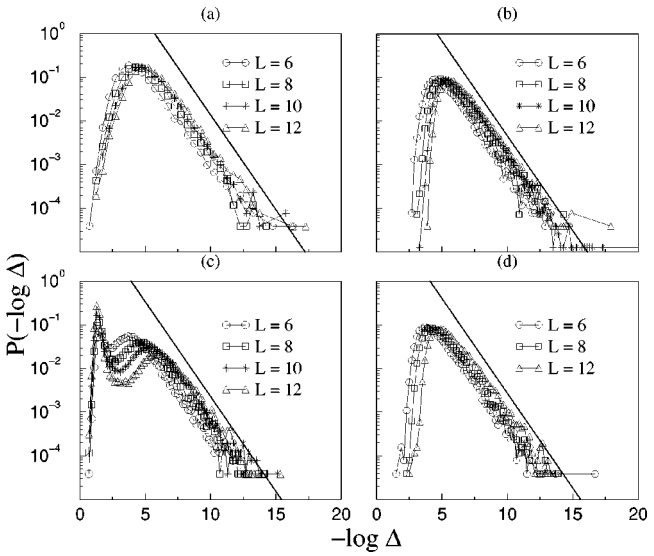

FIG. 10. Probability distribution of the energy gap on the cubic lattice with mixed F and AF bonds. (a) Gaussian distribution, $\sigma=1$; (b) symmetric rectangular distribution ($r=0$); (c) asymmetric rectangular distribution ($r=0.25$); (d) $S=1$ symmetric rectangular distribution. The low-energy tails of the gap distributions for all cases, indicated by straight lines, have a slope -1, corresponding to $\omega=0$.

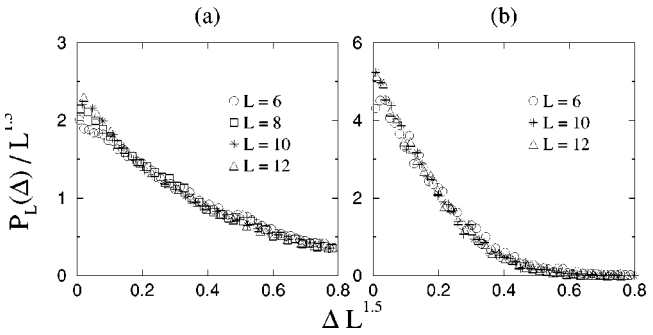

FIG. 11. Scaling of the reduced gap distribution, $\tilde{P}(L^z\Delta)=L^{-z}P_L(\Delta)$, for randomly frustrated 3D systems: (a) Gaussian randomness, $\sigma=1$ and (b) symmetric rectangular randomness. In both cases it is $z=1.5$.

As seen in Fig. 10 the slopes of the low-energy tail of the gap distributions are approximately constant, and for our finite systems they are consistent with a vanishing gap exponent

$$\omega \approx 0 \quad (d=3). \tag{25}$$

During renormalization, such as in the case of two dimensions, there is a large spin formation and the corresponding moment exponent is $\zeta=0.55$, for symmetric distributions (Gaussian and rectangular) and $\zeta=0.58$ for the asymmetric rectangular distribution. Thus ζ appears to be close to 1/2 in both cases. We have also studied the scaling behavior of the reduced gap distribution, $\tilde{P}(L^z\Delta)=L^{-z}P_L(\Delta)$. In Fig. 11 we show a scaling collapse of the distributions, which is obtained by $z\approx 1.5$ independently of the disorder distribution. The scaling curves seem to tend to a finite limiting value at $\Delta=0$, implying a gap exponent $\omega\approx 0$. We can thus conclude that—within the range of validity of the SDRG method—the relation in Eq. (13) is not valid for frustrated 3D models.

2. The J_1-J_2 model

We also considered frustration caused by a competition between nearest- and next-nearest-neighbor couplings in order to determine to what extent the universality of the spin-glass (SG) phase, observed in 2D models, is valid in three dimensions. Here we study systems at different points of the phase diagram, $J_2^{\max}/J_1^{\max}$, and for different initial disorder, D, using the same notations as those for two dimensions. Typical gap distributions are shown in Fig. 12, where we observe that the low-energy tail of the distributions in each case has approximately the same slope close to -1, which results in a gap exponent, $\omega\approx 0$. This result is consistent with Eq. (25) obtained for randomly frustrated models. During renormalization large spin formation is observed, and the moment exponent, ζ, is found to depend on the position in the phase diagram: for $J_2^{\max}/J_1^{\max}=0.5$ and 1.0 it is given by $\zeta=.58$ and .78, respectively ($D=1$ is in both cases). The dynamical exponent in these cases was about the same ($z\approx 3/2$) as for that of randomly frustrated models.

Thus we can conclude that also in three dimensions the low-energy fixed points of random Heisenberg systems with

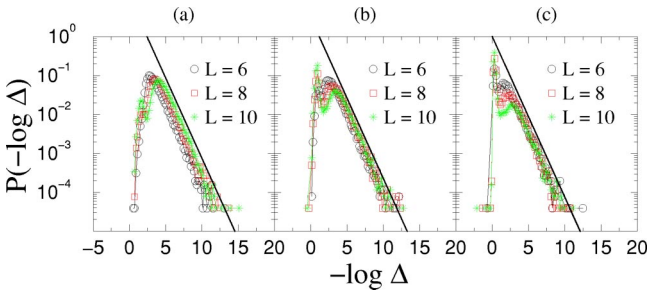

FIG. 12. Probability distribution of the energy gap of the J_1-J_2 model. (a) $J_2^{\max}/J_1^{\max}=0.5$, $D=1$; (b) $J_2^{\max}/J_1^{\max}=1$, $D=2$; (c) $J_2^{\max}/J_1^{\max}=1$, $D=1$. (The slope of the straight lines in all cases is -1.)

different types of frustration are controlled by the same type of SGFP, having the same gap exponent, $\omega \approx 0$, as in a two-dimensional SGFP. Therefore we conjecture that the ground states of these 3D frustrated models are in a spin-glass phase, too. At these SGFPs the dynamical exponent is constant, however, the moment exponent has a system dependence. Thus the low-energy excitations have a universal scaling behavior, but the thermodynamical singularities in Eq. (17), which depend on the value of ζ, are system dependent.

V. DISCUSSION

In this paper we considered higher-dimensional HAFs and studied the effect of strong randomness on their low-energy/low-temperature properties by a numerical application of the SDRG method. Comparing with the known, partially exact results for 1D HAFs we noticed several important differences. First, in higher dimensions one observes a strong universality scenario: there are only a few relevant fixed points (most important are the random AF fixed point and the SGFP) and their properties do not depend on the coordination number, the strength of disorder, value of the spin, etc., rather just on the dimension of the model and the degree of frustration in the system. In contrast to this, in random spin chains (with dimerization) and ladders one usually has a continuum of low-energy fixed points parametrized by the value of the dynamical exponent z and which do depend on the aforementioned details. Second, in higher-dimensional HAFs the singularities are controlled by (a few) conventional random fixed points, at which the dynamical exponent is finite. In higher-dimensional systems there are no IRFPs that can generally be found in (quasi)-1D systems at random quantum critical points. A third difference between 1D and higher-dimensional AFs is the following. In one dimension the renormalization of random spin-1/2 AF spin chains and random quantum ferromagnets, such as the random transverse Ising model,[7,8,41] leads to similar IRFPs at quantum critical points. In higher-dimensional random transverse Ising models the random quantum critical point is still an IRFP,[42,43] whereas for the random HAF, even at random quantum critical points, we found in this work the dynamical exponent to be finite.

One remarkable aspect of our results is the observed universality of the fixed point controlling the low-energy characteristics of random frustrated systems.[44] The gap exponent of this so-called spin-glass fixed point (SGFP) is numerically very close to zero[45] and we can explain this observation in the following way. During renormalization there is a large spin formation in these systems and therefore we expect that the low-energy excitations in $d \geqslant 2$ are extended over the whole (finite) volume of the system (in a 1D topology these excitations are not extended since unfavorable domains usually restrict the size of excitations). As a consequence these excitations can be considered as compact objects so that their reduced (scale-invariant) probability density $\tilde{P}(L^z\Delta) = L^{-z}P_L(\Delta)$ has no size dependence for a fixed small gap, Δ. This last statement is consistent with a vanishing gap exponent, $\omega=0$, according to Eq. (11) and is supported by the numerical results in Fig.11.

Finally we remark about the accuracy of the results obtained with the SDRG method. It is generally expected that the SDRG method leads to asymptotically exact relations concerning singularities and scaling functions at IRFPs.[7,41] However, the same type of asymptotic accuracy of the results is predicted at GFPs and checked numerically by the density-matrix renormalization-group method.[8] Therefore we expect the predictions of the SDRG method about LSFPs and the SGFP also to be correct. This expectation finds support in the results of numerical calculations for the 1D Heisenberg model with mixed F-AF couplings[46] and for the $\pm J$ square lattice HAF.[17] Nevertheless alternative calculations are necessary to check the validity of the predictions of our SDRG results.

ACKNOWLEDGMENTS

F.I. is grateful to G. Fáth for useful discussions. This work has been supported by a German-Hungarian exchange program (DAAD-MÖB), by the Hungarian National Research Fund under Grant Nos. OTKA TO34138, TO37323, MO28418, and M36803, by the Ministry of Education under Grant No. FKFP 87/2001, and by the Center of Excellence Grant No. ICA1-CT-2000-70029. Numerical calculations are partially performed on the Cray-T3E at Forschungszentrum Jülich.

[1] P. Fazekas, *Lecture Notes on Electron Correlations and Magnetism* (World Scientific, Singapore, 1999).

[2] E. Fradkin, *Field Theories of Condensed Matter Systems* (Addison-Wesley, Palo Alto, 1991).

[3] N.D. Mermin and H. Wagner, Phys. Rev. Lett. **17**, 1133 (1966).

[4] L.J. de Jongh, in *Magnetic Phase Transitions*, edited by M. Ausloos and R.J. Elliott (Springer, New York, 1983), p. 172.

[5] D.C. Johnston, J.P. Stokes, D.P. Goshorn, and J.T. Lewandowski, Phys. Rev. B **36**, 4007 (1987); S.-W. Cheong, A.S. Cooper, L.W. Rupp, Jr., and B. Batlogg, *ibid.* **44**, 9739 (1991); M. Corti, A.

Rigamonti, and F. Tabak, *ibid.* **52**, 4226 (1995).
[6] S.K. Ma, C. Dasgupta, and C.-K. Hu, Phys. Rev. Lett. **43**, 1434 (1979); C. Dasgupta and S.K. Ma, Phys. Rev. B **22**, 1305 (1980).
[7] D.S. Fisher, Phys. Rev. B **50**, 3799 (1994).
[8] F. Iglói, R. Juhász, and P. Lajkó, Phys. Rev. Lett. **86**, 1343 (2001); F. Iglói, Phys. Rev. B **65**, 064416 (2002).
[9] R.A. Hyman and K. Yang, Phys. Rev. Lett. **78**, 1783 (1997); C. Monthus, O. Golinelli, and Th. Jolicoeur, *ibid.* **79**, 3254 (1997); A. Saguia, B. Boechat, and M.A. Continentino, *ibid.* **89**, 117202 (2002).
[10] G. Refael, S. Kehrein, and D.S. Fisher, Phys. Rev. B **66**, 060402 (2002).
[11] R. Mélin, Y.-C. Lin, P. Lajkó, H. Rieger, and F. Iglói, Phys. Rev. B **65**, 104415 (2002).
[12] E. Westerberg, A. Furusaki, M. Sigrist, and P.A. Lee, Phys. Rev. Lett. **75**, 4302 (1995); Phys. Rev. B **55**, 12 578 (1997).
[13] E. Yusuf and K. Yang, Phys. Rev. B **67**, 144409 (2003).
[14] K. Kato, S. Todo, K. Harada, N. Kawashima, S. Miyashita, and H. Takayama, Phys. Rev. Lett. **84**, 4204 (2000).
[15] A.W. Sandvik, Phys. Rev. B **66**, 024418 (2002).
[16] Y. Nonomura and Y. Ozeki, J. Phys. Soc. Jpn. **64**, 2710 (1995).
[17] J. Oitmaa and O.P. Sushkov, Phys. Rev. Lett. **87**, 167206 (2001).
[18] A. Luther and I. Peschel, Phys. Rev. B **12**, 3908 (1975).
[19] F.D.M. Haldane, Phys. Lett. **93A**, 464 (1983).
[20] For a review, see E. Dagotto and T.M. Rice, Science **271**, 618 (1996).
[21] J.D. Reger and A.P. Young, Phys. Rev. B **37**, 5978 (1988).
[22] H. Neuberger and T.A.L. Ziman, Phys. Rev. B **39**, 2608 (1989).
[23] B. Bernu, P. Lecheminant, C. Lhuillier, and L. Pierre, Phys. Rev. B **50**, 10 048 (1994); L. Capriotti, A.E. Trumper, and S. Sorella, Phys. Rev. Lett. **82**, 3899 (1999); A.E. Trumper, L. Capriotti, and S. Sorella, Phys. Rev. B **61**, 11 529 (2000).
[24] C. Zeng and V. Elser, Phys. Rev. B **42**, 8436 (1990); J.T. Chalker and J.F.G. Eastmond, *ibid.* **46**, 14 201 (1992); P.W. Leung and V. Elser, *ibid.* **47**, 5459 (1993); P. Lecheminant, B. Bernu, C. Lhuillier, L. Pierre, and P. Sindzingre, *ibid.* **56**, 2521 (1997); C. Waldtmann, H.-U. Everts, B. Bernu, P. Sindzingre, C. Lhuillier, P. Lecheminant, and L. Pierre, Eur. Phys. J. B **2**, 501 (1998).
[25] S.E. Palmer and J.T. Chalker, Phys. Rev. B **64**, 094412 (2001).
[26] B. Canals, Phys. Rev. B **65**, 184408 (2002).
[27] B. Canals and C. Lacroix, Phys. Rev. Lett. **80**, 2933 (1998).
[28] H.J. Schulz, T.A.L. Ziman, and D. Poilblanc, J. Phys. I **6**, 675 (1996).
[29] F. Figueirido, A. Karlhede, S. Kivelson, S. Sondhi, M. Rocek, and D.S. Rokhsar, Phys. Rev. B **41**, 4619 (1989); E. Dagotto and A. Moreo, Phys. Rev. Lett. **63**, 2148 (1989); M.P. Gelfand, R.R.P. Singh, and D.A. Huse, Phys. Rev. B **40**, 10 801 (1989); R.R.P. Singh and R. Narayanan, Phys. Rev. Lett. **65**, 1072 (1990); H.J. Schulz and T.A.L. Ziman, Europhys. Lett. **18**, 355 (1992).
[30] M.S.L. du Croo de Jongh, J.M.J. van Leeuwen, and W. van Saarloos, Phys. Rev. B **62**, 14 844 (2000); O.P. Sushkov, J. Oitmaa, and Z. Weihong, *ibid.* **63**, 104420 (2001).
[31] M. Matsumoto, C. Yasuda, S. Todo, and H. Takayama, Phys. Rev. B **65**, 014407 (2002).
[32] In one dimension where at $\alpha=0$ there is only QLRO the system becomes dimerized for any small value of α, thus $\alpha_c=0$. Here the gap opens with an exponent $\nu=2/3$; M.C. Cross and D.S. Fisher, Phys. Rev. B **19**, 402 (1979).
[33] J. Sirker, A. Klümper, and K. Hamacher, Phys. Rev. B **65**, 134409 (2002).
[34] R. Mélin, Eur. Phys. J. B **16**, 261 (2000).
[35] F. Iglói, R. Juhász, and H. Rieger, Phys. Rev. B **61**, 11 552 (2000).
[36] R.B. Griffiths, Phys. Rev. Lett. **23**, 17 (1969).
[37] M.J. Thill and D.A. Huse, Physica A **15**, 321 (1995); H. Rieger and A.P. Young, Phys. Rev. B **54**, 3328 (1996); F. Iglói, R. Juhász, and H. Rieger, *ibid.* **59**, 11 308 (1999).
[38] C. Yasuda, S. Todo, M. Matsumoto, and H. Takayama, cond-mat/0204397 (unpublished).
[39] For a review see, e.g., H. Rieger and A.P. Young, *Quantum Spin Glasses*, *Lecture Notes in Physics*, in *Complex Behaviour of Glassy Systems*, edited by J.M. Rubi and C. Perez-Vicente (Springer-Verlag, Berlin, 1997), Vol. 492, p. 254.
[40] F. Mila, cond-mat/9805078 (unpublished).
[41] D.S. Fisher, Phys. Rev. Lett. **69**, 534 (1992); Phys. Rev. B **51**, 6411 (1995).
[42] O. Motrunich, S.-C. Mau, D.A. Huse, and D.S. Fisher, Phys. Rev. B **61**, 1160 (2000).
[43] Y.-C. Lin, N. Kawashima, F. Iglói, and H. Rieger, Prog. Theor. Phys. Suppl. **138**, 470 (2000); D. Karevski, Y.-C. Lin, H. Rieger, N. Kawashima, and F. Iglói, Eur. Phys. J. B **20**, 267 (2001).
[44] The numerical results obtained in Ref. 16 suggest that weakly frustrated systems, such as the randomly frustrated models in Sec. IV A 4 with a small fraction of F bonds, are still in the random HAF phase and not in the SG phase.
[45] A similar relation, $\omega=0$ and $z=d$, holds at the boson localization transition point: M.P.A. Fisher, P.B. Weichman, G. Grinstein, and D.S. Fisher, Phys. Rev. B **40**, 546 (1989); and in the Bose glass phase: J. Kisker and H. Rieger, Physica A **246**, 348 (1997). This singularity is controlled by a GFP, therefore its origin is different from that at the SGFP.
[46] T. Hikihara, S. Furusaki, and M. Sigrist, Phys. Rev. B **60**, 12 116 (1999).